

# Collective transport in locally asymmetric periodic structures

I. Derényi<sup>a)</sup>

Department of Surgery, MC 6035, University of Chicago, 5841 South Maryland Avenue, Chicago, Illinois 60637

P. Tegzes and T. Vicsek

Department of Atomic Physics, Eötvös University, Budapest, Puskin u 5-7, 1088, Hungary

(Received 27 February 1998; accepted for publication 29 June 1998)

In this paper we give an overview of the *cooperative effects* in fluctuation driven transport arising from the interaction of a large number of particles. (i) First, we study a model with finite-sized, overdamped Brownian particles interacting via hard-core repulsion. Computer simulations and theoretical calculations reveal a number of novel cooperative transport phenomena in this system, including the *reversal of direction of the net current* as the particle density is increased, and a very strong and *complex dependence of the average velocity* on both the size and the average distance of the particles. (ii) Next, we consider the cooperation of a collection of motors rigidly attached to a backbone. This system possesses *dynamical phase transition* allowing *spontaneous directed motion* even if the system is spatially symmetric. (iii) Finally, we report on an experimental investigation exploring the horizontal transport of granular particles in a vertically vibrated system whose base has a sawtooth-shaped profile. The resulting material flow exhibits complex collective behavior, both as a function of the number of layers of particles and the driving frequency; in particular, under certain conditions, increasing the layer thickness leads to a *reversal of the current*, while the *onset of transport* as a function of frequency occurs gradually in a manner reminiscent of a *phase transition*. © 1998 American Institute of Physics. [S1054-1500(98)02103-X]

**Recently there has been considerable interest in the various transport processes, often referred to as fluctuation driven transport, that take place in systems with no macroscopic driving forces. In the corresponding models, the transport of particles is sustained by nonequilibrium fluctuations in a periodic, locally asymmetric, but macroscopically flat structure. Motivated by numerous biological and physical systems, special attention has been paid to the cooperative effects arising from the interaction of a large number of such particles moving along the same structure. Here we outline some of the new collective phenomena occurring in different models and present the results of an experiment with granular materials moving in a vertically vibrating system with a sawtooth-shaped base.**

## I. INTRODUCTION

The most common and best known transport phenomena occur in systems in which there exist macroscopic driving forces (typically due to external fields or concentration gradients). However, recent theoretical studies have shown that far from equilibrium processes in structures possessing vectorial symmetry can bias thermal noise and induce macroscopic motion on the basis of purely microscopic effects.<sup>1-13</sup> This newly suggested mechanism is expected to be essential for the operation of molecular combustion motors that are responsible for many kinds of biological motion such as cellular transport or muscle contraction.<sup>14</sup> A transport mecha-

nism of this kind has also been experimentally demonstrated in simple physical systems<sup>15,16</sup> and can lead to new technological ideas such as designing nanoscale devices, constructing a novel type of particle separator, or treating solid surfaces.<sup>17</sup>

### A. Motion of a single particle

In the theoretical models, loosely termed “thermal ratchets,” Brownian particles are moving in an overdamped environment along one-dimensional asymmetric periodic potentials due to the effect of nonequilibrium fluctuations. For simplicity and illustration purposes let us choose the potential to be sawtooth shaped [Fig. 1(a)], and consider two basic types of fluctuations: the fluctuating potential [Fig. 1(b)] and the fluctuating force [Fig. 1(c)].

In the case of the fluctuating potential the sawtooth potential is switched on and off repeatedly with appropriate switching rates. Figure 1(b) illustrates the time evolution of the probability distribution of the position of the particle starting from one of the potential valleys. Due to a combination of diffusion during the “off” state and directed motion during the “on” state a net motion to the *left* can be observed.

When the effects of a fluctuating force  $F(t)$  are considered,  $F(t)$  is assumed to alternate between  $+F$  and  $-F$  with an appropriate characteristic frequency and with zero time average [Fig. 1(c)]. When the force points to the right [ $F(t) = +F$ ], the probability of jumping to the right dominates the jumping events with the coefficient  $\exp(-(\Delta E - F\lambda_1)/k_B T)$ . When the force is  $-F$ , the probability of jumping to the left dominates, but with the coefficient

<sup>a)</sup>Electronic mail: derenyi@rainbow.uchicago.edu

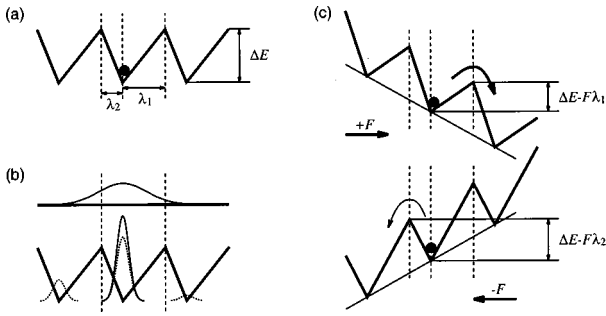


FIG. 1. The motion of a Brownian particle (a) in a sawtooth-shaped potential due to the effect of (b) fluctuating potential and (c) fluctuating force.

$\exp(-(\Delta E - F\lambda_2)/k_B T)$ . And since  $\lambda_1 > \lambda_2$ , this fluctuating force results in a net motion to the right.

**B. Transport of many interacting particles**

In the actual realizations of the ratchet mechanism typically there are many particles moving at the same time. Such systems include examples ranging from biology to physics. In the case of muscle contraction the motion is due to the simultaneous action of myosin molecules. In the dielectrophoretic experiments on the directed migration of small polystyrene beads the motion of many colloidal particles was studied.<sup>15</sup> It is a natural question to investigate whether the interaction among many particles leads to collective phenomena specific to the ratcheting mechanism.

One of the most interesting aspects of many particle systems is that they exhibit a complex cooperative behavior during phase transition. This remarkable feature of equilibrium systems has been studied in great detail for the last couple of decades leading to a deeper understanding of processes which may take place in an assembly of interacting particles. Concepts like scaling, universality, and renormalization have resulted in a systematic picture of a wide range of systems in physics.<sup>18,19</sup>

Remarkably, far-from-equilibrium systems of many particles have been shown to exhibit collective behavior as well. In particular, the existence of phase transition type behavior has been demonstrated in several investigations of growth phenomena.<sup>20-22</sup> These and further analogies with the basic features of equilibrium systems have represented a particularly important contribution to the understanding of the complex behavior of nonequilibrium processes.

Here we review recent results on the simultaneous motion of many particles moving in asymmetric structures in the presence of nonequilibrium fluctuations. In the related theoretical, numerical, and experimental studies novel kinds of transitions could be observed indicating that many interacting particles exhibit collective behavior in ratchet systems as well, although the nature of this behavior can be very specific and sometimes surprising.

**II. COLLECTIVE BEHAVIOR OF FINITE-SIZED PARTICLES**

In this section we discuss the collective motion of finite-sized Brownian particles in a one-dimensional sawtooth-

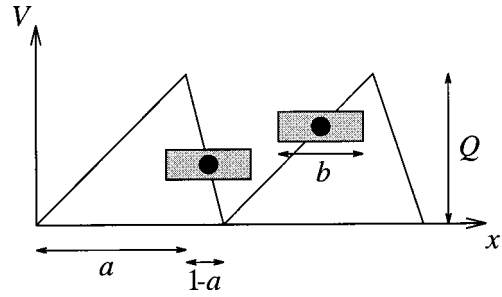


FIG. 2. Schematic picture of the system we consider showing two particles with size  $b$  subject to the sawtooth-shaped periodic potential  $V(x)$ . The period of the potential is  $\lambda = 1$ , where the lengths of the slopes are  $\lambda_1 = a$  and  $\lambda_2 = 1 - a$ . The potential difference between the top and the bottom is  $Q$ .

shaped potential for both fluctuating force<sup>23</sup> and fluctuating barrier.<sup>24</sup> The interaction between the particles has been supposed to be simple hard-core repulsion.

**A. Fluctuating driving force**

For fluctuating force the motion of each particle is described by the Langevin equation:

$$\dot{x}_j = -\partial_x V(x_j) + F_j(t) + \xi_j(t), \quad j = 1, \dots, N, \quad (1)$$

where  $N$  is the number of particles,  $x_j$  denotes the position of the center of mass of the  $j$ th particle,  $V(x)$  is a sawtooth-shaped periodic potential,  $F_j(t)$  is the fluctuating driving force with zero time average, and  $\xi_j(t)$  is Gaussian white noise with the autocorrelation function  $\langle \xi_j(t) \xi_i(t') \rangle = 2k_B T \delta_{j,i} \delta(t - t')$ . These equations are coupled by the hard-core repulsive interaction, i.e., by the constraint that neighboring particles are not allowed to overlap during their motion. All particles have the same size  $b$ , while the period of the potential is  $\lambda = 1$ , as shown in Fig. 2. The size of the system or in other words the number of the periods is  $L$  (and  $L$  go to infinity, while  $L/N$  remains finite).

Normally, one single particle moves in the direction corresponding to the smaller uphill slope of the potential. However, there is a range of the parameters of the periodic driving force for which the particle migrates into the opposite direction.<sup>6-9</sup> In this regime computer simulations revealed<sup>23</sup> that *gradual addition of particles* into the system *results in the change of their average velocity* back to the “normal” direction. We have tested this result for several different cases (including driving forces periodic in time<sup>7</sup> and distributed according to “kangaroo” statistics<sup>6</sup>) and we have found that this change of the current’s direction is a universal property of the collective motion in this model. Figure 3 shows a simple example, where the driving forces are  $F_j(t) = A \sin(\omega_j t)$  and the  $\omega_j$  values are chosen randomly around a fixed value  $\omega$  with a dispersion of several percentage of  $\omega$  (to avoid synchronization). The plot shows the average velocity as a function of  $\omega$ , for various values of the particle density defined as  $\rho = bN/L$  ( $0 < \rho < 1$ ). In the inset we have plotted the fundamental diagram: the particle current  $J = vN/L$  as a function of the particle density for  $\omega = 175$ .

Another interesting feature can be observed by *changing the size* of the particles while keeping the average distance

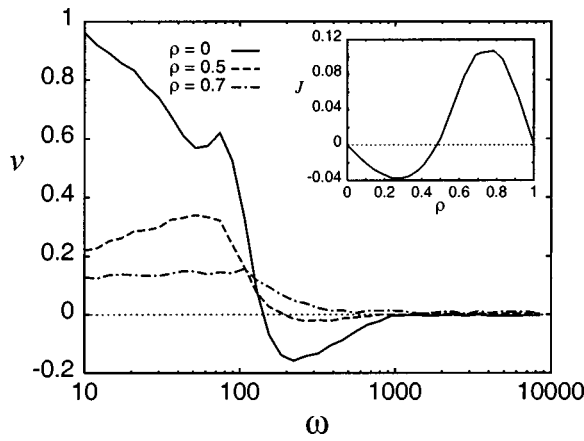


FIG. 3. The plot of the average velocity  $v$  as a function of the average frequency  $\omega$  of the sinusoidal driving forces for three different values of the particle density  $\rho = bN/L$ . The inset demonstrates the reversal of the particle current  $J \equiv vN/L$  as a function of the particle density  $\rho$ , for  $\omega = 175$ . ( $Q = 4$ ,  $a = 0.8$ ,  $b = 0.5$ ,  $T = 1$ , and the amplitude of the driving forces  $A = 32$ .)

between neighboring particles ( $s = L/N - b$ ) fixed: The average velocity shows a complex nonmonotonic dependence on the size of the particles, especially at small  $s$  (or high particle density). The smaller the average distance  $s$ , the more and the bigger the peaks appear around the rational values of  $b$ . Investigating the origin of this strange behavior we examine the simplest case when the driving force is *stationary*,  $F_j(t) = F$ , and smaller than the uphill gradient of the potential.

Let us consider the case when the size of the particles is somewhat *less* than 1 and there are two particles in the neighboring valleys of the potential. Then the second particle is not able to jump further ahead until the first one jumps away. So the first one hinders the second one. Thus the average velocity is smaller than the velocity of a single particle. Figure 4(a) shows this situation for 15 particles. A *vacancy type* current can be observed as a consequence of the traffic jams arising from the hindering of particles. This phenomenon is also related to jams common in one-dimensional driven diffusive systems and traffic models.<sup>25</sup> If the size of the particles is a bit *larger* than 1 and there are also two particles in the neighboring valleys, both of them cannot be in their minimum energy position at the same time, therefore, the first one has a larger chance to jump further. In this case the second one indirectly “pushes” the first one, however, the first one also hinders the second one. But in spite of the hindering effect, the average velocity can even be larger than the velocity of a single particle. This situation is shown in Fig. 4(b) for 12 particles. There are no jams and the density waves indicate that the particles help each other to jump through to the next valley. At high particle densities similar arguments hold for the explanation of the sensitive dependence of the average velocity on  $b$  around other rational values, too. In case of slowly alternating external forces these effects (hindering and pushing) are expected to influence the net transport.

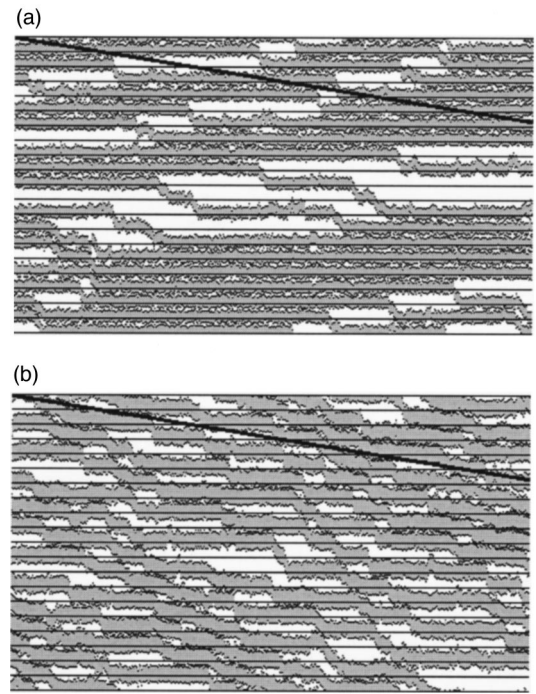


FIG. 4. Motion of the particles in the space–time domain. The time increases from left to right and the particles are moving downwards under the influence of the stationary driving force  $F$ . Horizontal lines represent the bottom of the potential valleys, and the wide slanted line represents the average motion of a single noninteracting particle. (a) Shows 15 particles with size  $b = 0.833$ . A vacancy type current can be observed, as a consequence of the hindering effect of particles. The average velocity  $v$  is smaller than the average velocity of one single particle. (b) Shows 12 particles with size  $b = 1.166$ . There are no jams, and the density waves show that the particles assist each other in jumping over to the next valley.  $v$  is larger than the velocity of a single particle. The average distance between particles is  $s = 0.5$  in both cases.

### B. Flashing potential

Next we study the motion of particles with hard-core repulsion, in an asymmetric potential that is switched on and off *at the same time for all the particles*.<sup>24</sup> This natural extension of the on/off model to many particles also leads to a rich phenomenology.

As before we consider  $N$  overdamped Brownian particles of size  $b$  moving on a segment of length  $L$ . They are submitted to a sawtooth periodic potential  $V(x, t)$ , which is periodically turned “on” for a time  $\tau_{\text{on}}$  and then “off” for a time  $\tau_{\text{off}}$ . Units are chosen so that again the potential spatial period  $\lambda$  is 1, as well as the friction coefficient of the particles. The asymmetry of the potential is characterized by the length  $\lambda_1 = a$ .

If  $x_j$  denotes the position of the (center of) particle  $j$ , the evolution of the system is then described by the Langevin equations:

$$\dot{x}_j = -\partial_x V(x_j, t) + \xi_j(t), \quad j = 1, \dots, N, \quad (2)$$

which are coupled by the constraint that neighbor particles are not allowed to overlap:  $(x_j - x_{j-1}) > b$ .

Let us investigate how the average velocity  $v$  of the particles depend on their size  $b$  and density  $\rho = bN/L$ , in the limit of large systems ( $N$  and  $L$  go to infinity while  $\rho$  remains finite). To get analytical solutions we focus on specific re-

gimes: First the pinning potential  $V_{on}$  is taken strong enough so that during the time  $\tau_{on}$  the particles drift quickly to the positions corresponding to the nearest local energy minimum of the system, where they get trapped. This deep potential valley limit ( $Q \gg k_B T$ ) furthermore suits fast separation purposes. Second,  $\tau_{off}$  is long enough for the particles to forget (modulo the period) their initial position on the sawtooth during an “off” period. The average displacement over a cycle is then that of initially randomly distributed particles during a single “on” phase.

In the low-density limit, a particle with random initial position in the  $[-\lambda_2, \lambda_1]$  period ends at  $x=0$  after an “off” phase. The average progression per cycle is thus  $\langle d \rangle = \frac{1}{2}(\lambda_2 - \lambda_1) = 1/2 - a$ . Let us now turn to the other extreme: an almost packed system  $\rho \approx 1$ .

Consider the limit case  $\rho = 1$ , where the system is equivalent to a single particle of size  $L$ , the position of which is measured by  $x_1$ , for example. In the incommensurate case ( $b$  irrational), the particles are uniformly distributed in the periods whatever the value of  $x_1$ , so the whole system feels a flat potential whether the sawtooth potential is “on” or “off.” Therefore the average velocity of the particles is zero. We now turn to the much richer commensurate case:  $b = n/m$  in irreducible form. The effective potential seen by the equivalent  $L$ -size particle during “on” periods is a sawtooth potential of period  $\lambda' = 1/m$  with two linear pieces of lengths  $\lambda'_1 = \{ma\}/m$  and  $\lambda'_2 = \{m(1-a)\}/m$  (the notation  $\{\cdot\}$  means the fractional part), and the barrier height is  $NQ'$ , where

$$Q' = Q \frac{\{ma\}\{m(1-a)\}}{ma \cdot m(1-a)}. \quad (3)$$

Applying the single particle limit to the equivalent particle, we get its average displacement per cycle (which is that of every real particle):

$$\langle d \rangle = \frac{1}{2} (\lambda'_2 - \lambda'_1) = \frac{1}{2m} (1 - 2\{ma\}). \quad (4)$$

It can be proven<sup>24</sup> that this result holds in that limit when  $N \rightarrow \infty$  is taken first and then  $\rho \rightarrow 1$ .

This leads to a quite strange behavior for the high-density ( $N \rightarrow \infty$ ,  $\rho = 1 - \epsilon$ ) drift as a function of the particles size as illustrated by Fig. 5. The limit average displacement per on-off cycle  $\langle d \rangle$  is an erratic, discontinuous function with sharp peaks [given by Eq. (4)] for rational values of  $b$ , and zero otherwise. Both positive and negative peaks are present, in a pattern that depends on the value of the asymmetry parameter  $a$ .

Remember that at zero particle density, the average displacement per cycle is positive (if  $a < 0.5$ ), and independent of the size of the particles. Increasing the density from 0 to 1, it evolves to the discontinuous function shown in Fig. 5. The question is how this occurs. When the density is still less than 1 the function  $\langle d(b) \rangle$  has to be continuous, due to the smoothing effect of the finite temperature. It can be shown<sup>24</sup> that increasing the density from 0 to 1 while keeping the

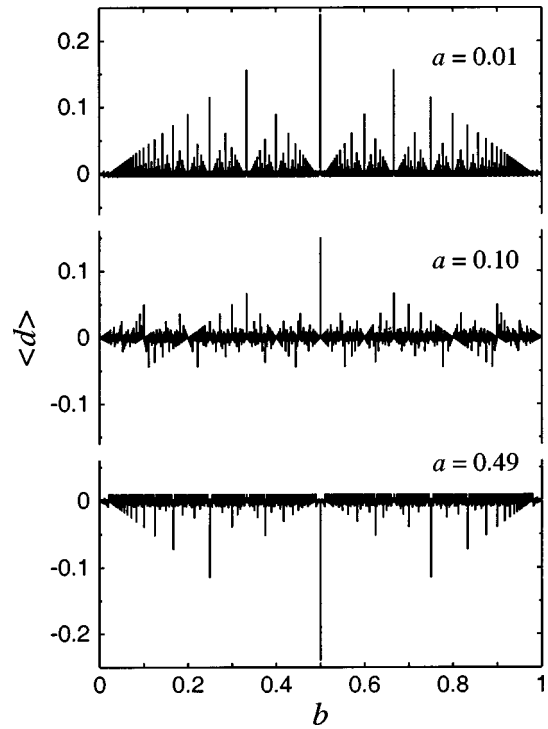


FIG. 5. High-density limit for the average particle displacement per on-off cycle  $\langle d \rangle$  as a function of the particles size  $b$ , for different values of the asymmetry parameter  $a$ .

particle size  $b$  fixed, the velocity can vary nonmonotonically and can even change sign several times, along a route that will be sensitive to the actual value of  $b$ .

### III. COLLECTIVE BEHAVIOR OF RIGIDLY ATTACHED PARTICLES

In several biological studies large groups of motor proteins are working together to transport relatively big objects. Jülicher and Prost<sup>26</sup> introduced a model to describe the behavior of these systems. In this model a large number of particles is subject to a periodic, asymmetric potential, that is turned “on” and “off” independently for each particle, and the particles are attached to a rigid backbone that keeps the distance between them fixed (Fig. 6).

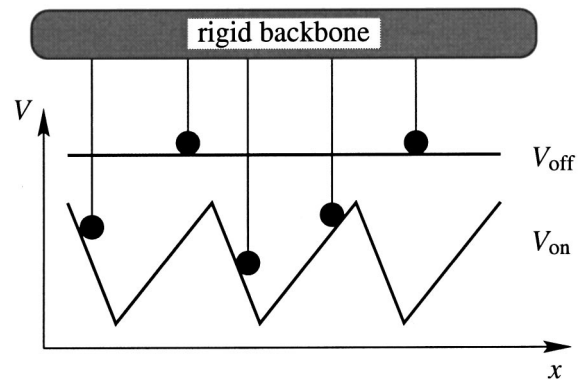


FIG. 6. Schematic representation of the two-state model with many particles attached to a rigid backbone.

In the following, we focus on the case where either the particles are randomly attached to the backbone or the spacing between them is constant but incommensurate with the period of the potential. In both cases the particles are uniformly distributed in the periods, and can be characterized by the probability distribution  $P_{\text{on}}(x,t)$  and  $P_{\text{off}}(x,t) = 1 - P_{\text{on}}(x,t)$ , where  $0 \leq x < 1$  denotes the particle position with respect to the potential period and ‘‘on’’ and ‘‘off’’ refer to the state of the potential.

The equations of motion for this system are<sup>26</sup>

$$\partial_t P_{\text{on}} + v \partial_x P_{\text{on}} = -\omega_{\text{on}}(x) P_{\text{on}} + \omega_{\text{off}}(x) P_{\text{off}}, \quad (5)$$

$$\partial_t P_{\text{off}} + v \partial_x P_{\text{off}} = +\omega_{\text{on}}(x) P_{\text{on}} - \omega_{\text{off}}(x) P_{\text{off}},$$

where  $\omega_{\text{on}}(x)$  and  $\omega_{\text{off}}(x)$  denote the transition rates between the two states of the potential, and the velocity of the backbone,  $v$ , is determined by  $v = f_{\text{ext}} + f$  (units are chosen again so that the friction coefficient is 1). The external force  $f_{\text{ext}}$  and the average force

$$f = - \int_0^1 dx (P_{\text{on}} \partial_x V_{\text{on}}(x) + P_{\text{off}} \partial_x V_{\text{off}}(x)) \quad (6)$$

exerted by the potentials (which should be zero for the flat potential) are normalized per particle.

In the steady state, using the relation  $P_{\text{off}} = 1 - P_{\text{on}}$ , these equations reduce to

$$v \partial_x P_{\text{on}} = -(\omega_{\text{on}}(x) + \omega_{\text{off}}(x)) P_{\text{on}} + \omega_{\text{off}}(x), \quad (7)$$

$$f_{\text{ext}} = v + \int_0^1 dx P_{\text{on}} \partial_x (V_{\text{on}}(x) - V_{\text{off}}(x)). \quad (8)$$

These equations allow the determination of the external force  $f_{\text{ext}}(v)$  that corresponds to a constant velocity  $v$ . Equation (8) can be solved either analytically for some potential shapes or in a power expansion as a function of the velocity  $v$ .<sup>26</sup>

Let us express  $\omega_{\text{on}}(x)$  as  $\omega_{\text{off}}(x) e^{(V_{\text{on}}(x) - V_{\text{off}}(x))/(k_B T) + \Omega \Theta(x)}$ , where now the ‘‘amplitude’’  $\Omega$  measures the distance from equilibrium (for  $\Omega = 0$  detailed balance holds). In order to discuss cooperative effects, we consider a system with no external force and with symmetric periodic potentials. Let the perturbation  $\Theta(x)$  be non-negative, also symmetric, and localized in the vicinity of the potential minimum (i.e., it differs from zero only in that region). It can be shown<sup>26</sup> that if  $\Omega$  is smaller than a critical value  $\Omega_c$ , the velocity of the backbone is zero, but for  $\Omega > \Omega_c$  the solution bifurcates to two stable solutions  $v = \pm v(\Omega)$ , while the  $v = 0$  solution becomes unstable. Therefore a *continuous onset of motion* occurs at  $\Omega = \Omega_c$  via *spontaneous symmetry breaking*.

This spontaneous symmetry breaking can be understood qualitatively as follows. For  $v = 0$  the localized excitation  $\Omega \Theta(x)$  leads to a depletion of  $P_{\text{on}}(x)$  near the potential minimum. Since  $\Theta(x)$  and the potentials are spatially symmetric, the force  $f$  vanishes. If the system is now perturbed in such a way that the backbone moves to the right with a small velocity  $v$ , the depletion of  $P_{\text{on}}(x)$  is being transported to the right. Now the population along the positive potential slope is depleted, while along the negative slope it has gained par-

ticles. As a result, the average force  $f$  pulls the backbone to the right and increases the effect of the initial perturbation.

If the potential is asymmetric the spontaneous symmetry breaking transition is no longer possible, since the velocity is nonzero at zero external force for any nonvanishing excitation  $\Omega$ . However, if  $\Omega > \Omega_c$  two stable solutions for the velocity can still exist, and by changing the external force  $f_{\text{ext}}$  the transition between the two solutions is discontinuous and exhibits hysteresis.

Another version of this model, where the backbone is elastically coupled to its environment, leads to the onset of spontaneous oscillation instead of unidirectional motion.<sup>27</sup>

The condition of the backbone’s rigidity can be relaxed by assuming that the particles are attached via springs. In such models weakening the interaction between the particles allows us to study the crossover from single to collective motion.<sup>28</sup>

#### IV. HORIZONTAL TRANSPORT IN VERTICALLY VIBRATED GRANULAR LAYERS

These studies of the collective motion of particles in an asymmetric, periodic structure and the interesting new results for flows in excited granular materials<sup>29–34</sup> motivated us to carry out a series of experiments that explore the manner in which granular particles are *horizontally* transported by means of *vertical* vibration.

The investigation of a transport mechanism for granular materials analogous to that of ratchets is an appealing idea, both conceptually and practically. By carrying out experiments on granular materials vibrated vertically by a base with a sawtooth profile, it is possible to achieve a fascinating combination of two topics of considerable current interest, ratchets and granular flows. A number of recent papers have focused on vibration-driven granular flow, and the details of the resulting convection patterns have been examined, both by direct observation<sup>30,31,33,34</sup> and by magnetic resonance imaging.<sup>32,35</sup> Granular convection has also been simulated numerically by several groups; the study most closely related to the present work deals with the horizontal transport that occurs when the base is forced to vibrate in an asymmetric manner.<sup>36</sup>

Here we describe an investigation of the horizontal flow of granular material confined between two upright concentric cylinders undergoing vertical vibration. In order to induce transport, the height of the annular base between the cylinders has a periodic, piecewise-linear profile (in other words, it is sawtooth-like). We observe novel collective behavior in the resulting material flow, both as functions of the number of particle layers and the driving frequency. The most conspicuous features, for the experimental parameters used here, are that increasing the layer thickness results in a *reversal* of the current, and that the onset of transport as a function of frequency takes place in a manner analogous to a phase transition with an exponent  $\beta \approx 1.8$ .

#### A. Experiments

Figure 7 shows a schematic view of the experimental apparatus. To achieve a quasi-two-dimensional system without boundaries in the direction of the expected flow the

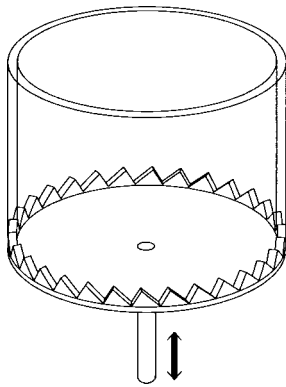


FIG. 7. Diagram of the experimental apparatus. The granular material is placed between the two glass cylinders and the whole assembly is subjected to sinusoidal vertical vibration.

granular material is placed between two concentric glass cylinders.<sup>33</sup> The mean diameter of the cylinders is 10 cm, while the gap between the cylinders is either 3 or 5 mm. A ring filling the gap between the cylinders, with a sawtooth profile on its upper surface, is mounted on the base of the container; the ring is made of either PVC (“soft”) or danamid (“hard”), and different sawtooth shapes are used. The entire assembly is vertically vibrated with a displacement that depends sinusoidally on time.

The apparatus has a strong steel framework and is fixed upon a heavy concrete base in order to reduce unintended vibrations. However, these precautions do not affect the rotational vibrations of the cylinders around their axis, which can lead to dramatic experimental artifacts. They have been eliminated by a horizontal steel rod fastened to the cylinders. The two ends of the rod are closely fitted to vertical plates allowing vertical but suppressing horizontal motion. The vertical vibration of the system is provided by an electromotor placed below the cylinders. The rotation of the motor is converted into vibration by an excenter, and its frequency is controlled by the following method. A disk with 20 holes around its perimeter is fixed to the rotating shaft of the motor and the light passing through the holes is detected by a photocell. The sign of the photocell is negatively fed back to the motor resulting in a stable frequency. In order to make the load of the motor uniform a counterweight is also fixed to the rotating shaft.

Our arrangement is naturally different from the real two-dimensional case because of the existence of the sidewalls. They certainly affect the motion of the particles by increasing dissipation and by inducing rotation of the particles. We believe, however, that these effects only slightly modify and do not change qualitatively our results.

Two types of granular media are used in the experiments, monodisperse glass balls and quasiellipsoidal plastic beads (see the inset of Fig. 8). The glass balls are nearly spherical with a diameter of  $3.3 \text{ mm} \pm 2\%$ . The plastic beads have a much greater size dispersion: two of the axes are approximately equal in length and lie in the range 2.4–3.0 mm, while the third axis is 1.2–1.7 mm. As shown in the inset of Fig. 8, the size of each sawtooth is similar to that of the particles. Two sawtooth shapes are considered; in one

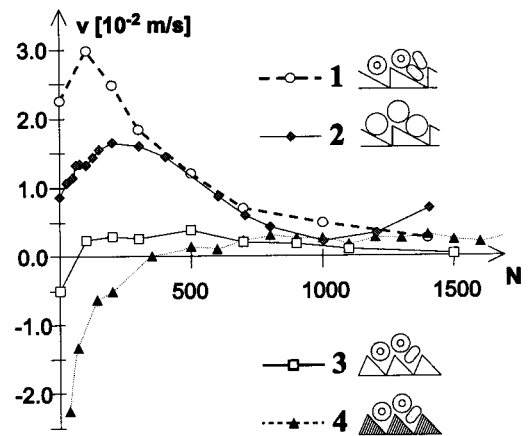


FIG. 8. Horizontal velocity as a function of the number of particles. The four curves represent measurements for different sawtooth shapes and materials and for different particle types: (1) strongly asymmetric sawtooth-shaped PVC and plastic beads; (2) strongly asymmetric sawtooth-shaped PVC and glass balls; (3) weakly asymmetric sawtooth-shaped PVC and plastic beads; (4) weakly asymmetric sawtooth-shaped danamid and plastic beads. The amplitude and frequency are  $A = 2 \text{ mm}$ ,  $f = 25 \text{ Hz}$ .

case the ratio of the horizontal projection of the tooth edges is 1:2 (“weak” asymmetry), in the other the left-hand edge is vertical (“strong” asymmetry).

Provided the frequency is sufficiently large, the vertical vibration causes horizontal flow of the entire granular layer. This bulk motion is reproducible over repeated experiments. The average flow velocity is determined by tracking individual tracer particles visible through the transparent cylinder walls. In order to average out fluctuations, the particles are allowed to travel large distances; depending on the size of the fluctuations this distance is between 1.5 and 6 m (equal to 5–20 times the circumference of the system). Each point shown in the graphs is an average over 3–6 tracer particles.

The typical trajectory of a single tracer particle is shown in Fig. 9. These data points were measured by using 200 glass balls and a strongly asymmetric sawtooth-shaped PVC base, and applying a vibration with frequency  $f = 25 \text{ Hz}$  and amplitude  $A = 2 \text{ mm}$ . In this case the motion of the tracer particle is nearly uniform, but some variation of velocity can be clearly seen. The two breaks in the curve correspond to occasional big jumps of the particle in the negative direction. Decreasing the number of particles these backward jumps become more frequent.

The tracer particles have to be chosen carefully to avoid segregation effects. Our tracers were identical to the other particles except for their colors. The plastic beads are available in many colors, but in the case of glass balls we had to dye them. In most cases we used alcohol-based pens for coloring, so that the surface properties of the balls changed as little as possible. We also used colored lacquer too, but because it produces a thicker layer on the surface we always tested the results with particles colored by alcohol-based pens.

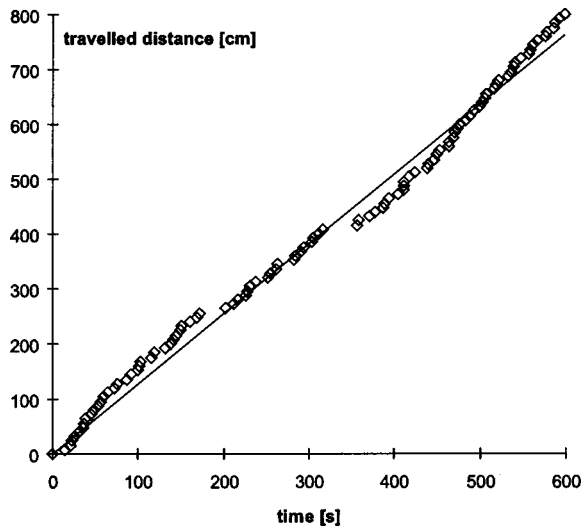


FIG. 9. Typical trajectory of a tracer particle: the advanced distance as a function of time. The continuous line is a linear fit. Strongly asymmetric sawtooth-shaped PVC was used with 200 glass balls. The amplitude and frequency were  $A=2$  mm,  $f=25$  Hz.

**B. Results**

Figure 8 shows the horizontal flow velocity as a function of the number of particles for four different versions of the system. The actual sawtooth and particle shapes are shown in the inset: curves 1 and 2 correspond to strongly asymmetric sawtooth shapes and different particle types, while curves 3 and 4 involve weak asymmetry and different base materials. Positive velocities are defined to be in the direction for which the left-hand edge of the sawtooth has the steeper slope. The vibration amplitude and frequency are  $A=2$  mm and  $f=25$  Hz; the dimensionless acceleration  $\Gamma=(2\pi f)^2 A/g$  is an important quantity for vibrated granular systems, so that here  $\Gamma=5$ .

The most striking difference between the curves is due to the different sawtooth shapes. While the velocities in curves 1 and 2 are always positive, curves 3 and 4 begin negative and only later become positive, in other words, even

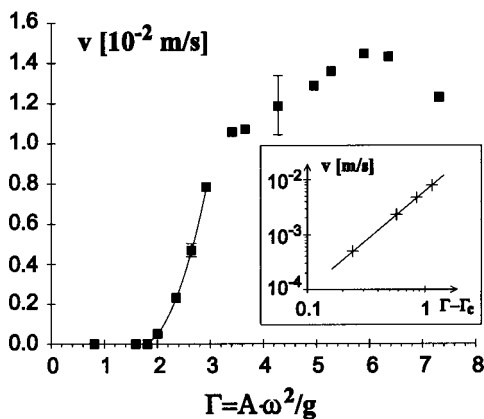


FIG. 10. Horizontal velocity  $v$  as a function of the dimensionless acceleration  $\Gamma$  at constant amplitude ( $A=2$  mm). The experiment is for a strongly asymmetric sawtooth-shaped PVC and 200 glass balls. The inset shows a log-log plot of  $v$  close to the transition as a function of  $\Gamma-\Gamma_c$ , where  $\Gamma_c=1.75$ .

the flow *direction* depends on the layer thickness. Additionally, the well-defined maxima in the first two curves are not present in curves 3 and 4. Altering the particle shape reduces the velocity and shifts the location of the maximum, but the shape of the curve remains unchanged. Likewise, changing the elasticity of the base does not alter the curve qualitatively. The different curves do nevertheless have certain features in common. For thin layers (corresponding to a small number of particles) they all begin with positive slope. Furthermore, for the thicker layers (larger numbers of particles), the velocity is always positive.

Figure 10 shows the  $\Gamma$  dependence of the flow velocity for a system of 200 balls (amounting to four layers) for constant  $A$ ; this graph corresponds to the experimental system shown in curve 2 of Fig. 8 (glass balls and strongly asymmetric sawtooth-shaped PVC). Flow occurs only above a critical acceleration  $\Gamma_c \approx 1.75$ . Slightly above this critical value the velocity appears to follow a power law

$$v(\Gamma) \propto (\Gamma - \Gamma_c)^{1.8}, \tag{9}$$

suggesting that the onset of flow resembles the kind of phase transition observed at a hydrodynamic instability such as thermal convection.<sup>37</sup>

**ACKNOWLEDGMENTS**

This work was supported in part by Grants No. OTKA T019299 and No. FKFP 0203/1997.

<sup>1</sup>A. Ajdari and J. Prost, *C. R. Acad. Sci. Paris* **315**, 1635 (1992).  
<sup>2</sup>M. O. Magnasco, *Phys. Rev. Lett.* **71**, 1477 (1993).  
<sup>3</sup>R. D. Astumian and M. Bier, *Phys. Rev. Lett.* **72**, 1766 (1994).  
<sup>4</sup>J. Prost, J.-F. Chauwin, L. Peliti, and A. Ajdari, *Phys. Rev. Lett.* **72**, 2652 (1994).  
<sup>5</sup>C. S. Peskin, G. B. Ermentrout, and G. F. Oster, in *Cell Mechanics and Cellular Engineering*, edited by V. Mow *et al.* (Springer, New York, 1994).  
<sup>6</sup>C. R. Doering, W. Horsthemke, and J. Riordan, *Phys. Rev. Lett.* **72**, 2984 (1994).  
<sup>7</sup>R. Bartussek, P. Hänggi, and J. G. Kissner, *Europhys. Lett.* **28**, 459 (1994).  
<sup>8</sup>M. M. Millonas and D. I. Dykman, *Phys. Lett. A* **185**, 65 (1994).  
<sup>9</sup>R. Bartussek, P. Reimann, and P. Hänggi, *Phys. Rev. Lett.* **76**, 1166 (1996).  
<sup>10</sup>R. D. Astumian and M. Bier, *Biophys. J.* **70**, 637 (1996).  
<sup>11</sup>P. Hänggi and R. Bartussek, in *Nonlinear Physics of Complex Systems*, edited by J. Parisi *et al.*, Lecture Notes in Physics (Springer, Berlin, 1996), Vol. 476, pp. 294–308.  
<sup>12</sup>R. D. Astumian, *Science* **276**, 917 (1997).  
<sup>13</sup>F. Jülicher, A. Ajdari, and J. Prost, *Rev. Mod. Phys.* **69**, 1269 (1997).  
<sup>14</sup>See, for example, B. G. Levi, *Phys. Today* **48**(4), 17 (1995).  
<sup>15</sup>J. Rousselet, L. Salome, A. Ajdari, and J. Prost, *Nature (London)* **370**, 446 (1994).  
<sup>16</sup>L. P. Faucheux, L. S. Bourdieu, P. D. Kaplan, and A. J. Libchaber, *Phys. Rev. Lett.* **74**, 1504 (1995).  
<sup>17</sup>I. Derényi, C. Lee, and A. L. Barabási, *Phys. Rev. Lett.* **80**, 1473 (1998).  
<sup>18</sup>H. E. Stanley, *Introduction to Phase Transitions and Critical Phenomena* (Oxford University Press, Oxford, 1971).  
<sup>19</sup>See, for example, S.-K. Ma, *Statistical Mechanics* (World Scientific, Singapore, 1985); *Modern Theory of Critical Phenomena* (Benjamin, New York, 1976).  
<sup>20</sup>*Surface Disordering*, edited by R. Jullien, J. Kertész, P. Meakin, and D. Wolf (Nova Science, New York, 1992).  
<sup>21</sup>N. Martys, M. Cieplak, and M. O. Robbins, *Phys. Rev. Lett.* **66**, 1058 (1991).

- <sup>22</sup>Z. CsaHók, K. Honda, E. Somfai, M. Vicsek, and T. Vicsek, *Physica A* **200**, 136 (1993).
- <sup>23</sup>I. Derényi and T. Vicsek, *Phys. Rev. Lett.* **75**, 374 (1995).
- <sup>24</sup>I. Derényi and A. Ajdari, *Phys. Rev. E* **54**, R5 (1996).
- <sup>25</sup>M. R. Evans, D. P. Foster, C. Godrèche, and D. Mukamel, *Phys. Rev. Lett.* **74**, 208 (1995).
- <sup>26</sup>F. Jülicher and J. Prost, *Phys. Rev. Lett.* **75**, 2618 (1995).
- <sup>27</sup>F. Jülicher and J. Prost, *Phys. Rev. Lett.* **78**, 4510 (1997).
- <sup>28</sup>Z. CsaHók, F. Family, and T. Vicsek, *Phys. Rev. E* **55**, 5179 (1997).
- <sup>29</sup>H. M. Jaeger, S. R. Nagel, and R. P. Behringer, *Rev. Mod. Phys.* **68**, 1259 (1996).
- <sup>30</sup>S. Douady, S. Fauve, and C. Laroche, *Europhys. Lett.* **8**, 621 (1989).
- <sup>31</sup>E. Clément, J. Duran, and J. Rachjenbach, *Phys. Rev. Lett.* **69**, 1189 (1992).
- <sup>32</sup>E. E. Ehrichs, H. M. Jaeger, G. S. Karczmar, J. B. Knight, V. Yu. Kuperman, and S. R. Nagel, *Science* **267**, 1632 (1995).
- <sup>33</sup>H. K. Pak and R. P. Behringer, *Phys. Rev. Lett.* **71**, 1832 (1993).
- <sup>34</sup>J. B. Knight, H. M. Jaeger, and S. R. Nagel, *Phys. Rev. Lett.* **70**, 3728 (1993).
- <sup>35</sup>M. Nakagawa, S. A. Altobelli, A. Caprhan, E. Fukushima, and E-K. Jeong, *Exp. Fluids* **16**, 54 (1993).
- <sup>36</sup>J. A. C. Gallas, H. J. Herrmann, and S. Sokolowski, *J. Phys. II* **2**, 1389 (1992).
- <sup>37</sup>P. Bergé and M. Dubois, *Contemp. Phys.* **25**, 535 (1984).